J Mol Model (2010) 16:1519–1527
DOI 10.1007/s00894-010-0669-9

ORIGINAL PAPER

Hydrogen-mediated Stone-Wales isomerization of dicyclopenta[*de,mn*]anthracene

Sonja Stanković · Svetlana Marković · Ivan Gutman · Silva Sretenović

Received: 4 November 2009 / Accepted: 18 January 2010 / Published online: 21 February 2010

Abstract The mechanism of transformation of two radicals (R1p and R1i) obtained by addition of a hydrogen atom to an external and internal carbon atom of dicyclopenta[*de,mn*] anthracene (P1) was investigated. Two pathways were revealed. The first mechanism is a one-step process, whereas the second mechanism includes two transition states and a cyclobutyl intermediate. The formation of R1p and R1i and the homolytic cleavage of the radicals obtained during the isomerization processes were also examined. In both pathways the addition of a hydrogen atom to the internal carbon significantly lowers the activation energy for hydrogen-mediated isomerization of P1 to acefluoranthene. This finding could be explained by the specific electronic structures of the transition states and intermediates participating in the isomerization processes.

Keywords Activation energy lowering · Density functional theory · Electronic structure · Radical mechanism

Electronic supplementary material The online version of this article (doi:10.1007/s00894-010-0669-9) contains supplementary material, which is available to authorized users.

S. Stanković · S. Marković (✉) · I. Gutman · S. Sretenović
Faculty of Science, University of Kragujevac,
12 Radoja Domanovića,
34000 Kragujevac, Serbia
e-mail: mark@kg.ac.rs

S. Stanković
Department of Organic Chemistry, Faculty of Bioscience Engineering, Ghent University,
Coupure Links 653,
9000 Ghent, Belgium

Introduction

Polycyclic aromatic compounds (PAHs) are generated during incomplete combustion of hydrocarbon-containing materials. They are considered as environmental pollutants, and some of them are responsible for the genotoxicity of combustion products. The genotoxicity of these PAHs is attributed to their specific structure, which usually includes the presence of five-membered rings (CP-PAHs) [1–3]. It was found that at high temperatures CP-PAHs undergo various isomerization and intraconversion processes, whereas many other reactions do not even occur [4–11]. It was suggested that CP-PAHs, when exposed to high temperatures, undergo consecutive ring-contraction/ring expansion processes, involving 1,2-C/1,2-H shifts [5, 8–12]. In addition, CP-PAHs have been a subject of numerous graph-theoretical [13, 14], semiempirical [5, 10, 11] and density functional theoretical (DFT) [11, 15, 16] investigations.

Scott et al. performed a series of flash vacuum pyrolisis (FVP) [17] experiments aimed at preparing dicyclopenta [*de,mn*]anthracene (P1) under various experimental conditions [4]. However, the products of these reactions were always mixtures of isomeric dicyclopenta[*de,kl*]anthracene (P2) and dicyclopenta[*jk,mn*]phenanthrene (P3). It was suggested that P1 did form, but, due to its instability, it underwent isomerization to P2 *via* ethynylaceanthrylene (I0) [4] (Fig. 1).

This assumption was recently confirmed using a DFT approach [18]. It was found that I0 can be transformed to both P1 and P2. The energetics of the investigated reactions indicates that P1 isomerizes to P2. The mechanism for a P2→P3 transformation is based on a ring contraction/ring conversion process, and requires extremely high temperatures. A mechanistic pathway for the P1→P3 isomerization was also revealed [19]. This transformation involves rear-

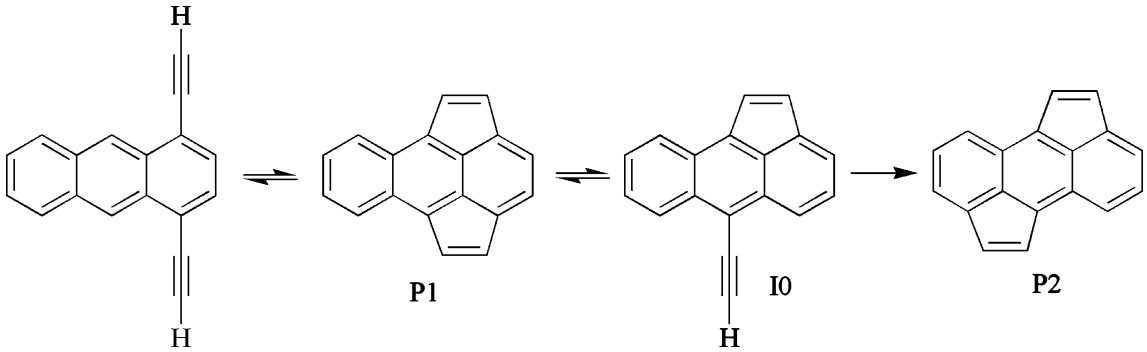

Fig. 1 Formation of dicyclopenta[*de,mn*]anthracene (P1) from 1,4-diethynylanthracene, and its isomerization into dicyclopenta[*de,kl*]anthracene (P2) *via* ethynylaceanthrylene (I0)

rangements of some hydrogen atoms and ring contraction/ring expansion. It was shown that the P1→P3 intraconversion is energetically more favorable than the P1→ P2 isomerization. All these facts indicate that, though P1 is unstable and reactive, it is an important intermediate in a variety of isomerization reactions.

The pyracylene-type isomerization (Stone-Wales rearrangement) is a transformation where a simultaneous rearrangement of two carbon atoms occurs. The Stone-Wales rearrangement was originally proposed as a hypothetical mechanism useful for deriving fullerene isomers [20]. Various mechanisms have been proposed for the Stone-Wales transformation [21–28]. Murry et al. found that the appearance of sp^3 carbon and 7-membered rings plays a central role in both the annealing and fragmentation process [21]. Their theoretical prediction indicates that the Stone-Wales rearrangement can occur *via* a nearly planar transition state, and *via* a non-planar intermediate which has one sp^3 and one sp hybridized carbon. The in-plane process, where two bonds are broken simultaneously, requires significantly higher activation energy than the one that involves two sequential 1,2 carbon shifts. Eggen et al. examined the Stone-Wales transformation in fullerene (C_{60}), and in the structures (C_{61}) obtained by addition of a carbon atom above the hexagon-hexagon and hexagon-pentagon fusion bonds [24]. They found that the energy barrier for the formation of the in-plane transition state was significantly reduced in the presence of an extra carbon atom. Novel investigations on the Stone-Wales rearrangement focus on non-planar transition states and intermediates, as they are energetically more favorable. Slanina et al. investigated catalytic effects of various atoms, both metals and non-metals, on the kinetics of the non-concerted Stone–Wales fullerene transformation, and pointed out that nitrogen and hydrogen atoms are particularly potent catalytic agents [25]. In addition, a study on a possible catalytic role of the CN radical in the Stone-Wales fullerene isomerization was put forward [27]. It was found that the reduction of the activation barrier due to the catalytic action of the CN radical is modest in comparison to a free nitrogen atom. Nimlos et al. [28] pointed out two mechanisms for the Stone-Wales rearrangement of pyracylene. The first mechanism occurs *via* a cyclobutyl intermediate, and the second contains one transition state with an sp^3-hybridized carbon atom. Hydrogen-mediated Stone-Wales isomerization of pyracylene was also examined. It was shown that the addition of a hydrogen atom to certain positions of pyracylene decreases the activation energy of the Stone-Wales rearrangement.

In a recent paper the mechanism of the Stone-Wales isomerization of P1 to acefluoranthene (P4) was investigated [29]. It was shown that the Stone-Wales rearrangement would require an extremely high activation energy, indicating that this isomerization process can occur only under a drastic temperature regime. The aim of this paper is to examine the possibility of extending the application of hydrogen-mediated Stone-Wales rearrangement to the isomerization of some radicals issued from P1. We assume that the addition of hydrogen atom to P1 can occur when a reaction mixture that produces P1 as an intermediate is exposed to flames, as it is known that flame environment consists of PAHs, small unsaturated hydrocarbons, carbon monoxide, hydrogen, and various free radicals, including hydrogen atoms at significant concentrations [30]. It is expected that a detailed analysis of the electronic structure of the transition states and intermediates can explain the possible decrease of the activation energy for hydrogen-mediated Stone-Wales rearrangement of P1.

Computational methods

In order to achieve compatibility of the results of the present work with the findings of our previous investigations [18, 19], we used the same computational method. Thus, geometrical parameters of all stationary points and transition states for the hydrogen atom mediated Stone-

Wales isomerization of dicyclopenta[*de,mn*]anthracene were optimized in vacuum, at the B3LYP/6-311G(d,p) level of theory [31–33], using the GAUSSIAN 03 W, version 6.1 program package [34]. The suitability of this level of theory for studies of reactions involving arenes, carbenes, and hydrocarbon free radicals has been previously established [18, 19, 28]. The unrestricted scheme for open-shell calculations of radical species was used. All calculated structures were verified to be local minima (all positive eigenvalues) for ground state structures, or first-order saddle points (one imaginary vibrational frequency) for transition state structures, by frequency calculations. From the transition structures, the intrinsic reaction coordinates (IRCs) were obtained using the IRC routine in Gaussian [35]. The natural bond orbital (NBO) analysis [36] was performed for all structures, using the GenNBO 5.0 program [37].

Results

There are nine different sites in P1 where hydrogen atom can be added. We examined the Stone-Wales rearrangement of two radicals, R1p and R1i. R1p and R1i are obtained by addition of a hydrogen atom to a carbon that lies on the perimeter of P1 (C3), and to an internal carbon atom (C18), respectively. The calculated structures of these radicals are depicted in Fig. 2.

Both radicals deviate from planarity due to the presence of sp^3 hybridized carbon atoms. G_{298} of R1i is lower than that of R1p by 41.41 kJ mol^{-1}. The SOMOs of the radicals (Fig. 1 in Online Resource 1) show that the unpaired electrons are delocalized over the carbon skeletons, and in the case of R1p a significant contribution to the SOMO also comes from H. The spin density maps of the radicals (Fig. 1 in Online Resource 1) indicate the sites with the highest spin density values. These maps are in accord with the NBO analysis that reveals that the spin density is distributed among C4 (0.392), C6 (0.438), C8 (0.130), C10 (0.094), C12 (0.102), C17 (0.066), and H (0.034) in R1p, and among C4 (0.187), C6 (0.238), C8 (0.283), C10 (0.254), C12 (0.133), and C13 (0.144) in R1i.

As in the case of the Stone-Wales rearrangement of P1 [29], two mechanistic pathways for the isomerization of R1p and R1i were revealed. The first mechanism is a concerted one-step process (pathway A), whereas the second mechanism includes two transition states and a cyclobutyl intermediate (pathway B). A reaction path for the rearrangement *via* a traditional Stone-Wales transition state was not revealed. It is worth pointing out that Nimlos et al. [28] were also unsuccessful in their attempts to obtain a transition state of C_2 symmetry. The formation of R1p and R1i and homolytic cleavage of the radicals obtained during the isomerization processes are included in pathway A. The Cartesian coordinates for the optimized geometries of all investigated species are provided in Online Resource 2.

Pathway A

The scheme of the mechanism is presented in Fig. 3. The energetic diagram of the reactions is shown in Fig. 4. The optimized geometries of all transition states in pathway A are depicted in Fig. 5. The selected bond lengths of the reactants, intermediates, transition states, and products are given in Table 1, whereas the values of the total energies, enthalpies and free energies are provided in Tables 1 and 2 in Online Resource 1.

Our investigations show that the formation of R1p and R1i from P1 and hydrogen atom occurs *via* transition states TS1p and TS1i (Figs. 3 and 4), requiring the activation energies of 51.0 and 44.8 kJ mol^{-1}, respectively (Tables 1 and 2 in Online Resource 1). Here, and throughout the text, an activation energy is calculated as the difference in free energy between a transition state and the corresponding reactant(s). In these transition states the carbon atoms almost lie within a plane (Fig. 5 and Online Resource 2) since C3 in TS1p and C18 in TS1i are sp^2 hybridized carbons. Spin density is distributed among C4, C6, and H in both transition states (0.196, 0.127, and 0.798 in TS1p; and 0.173, 0.116, and 0.818 in TS1i).

In TS2p (Fig. 5 and Online Resource 2) a simultaneous cleavage of the C4–C18 and C10–C17 bonds, and

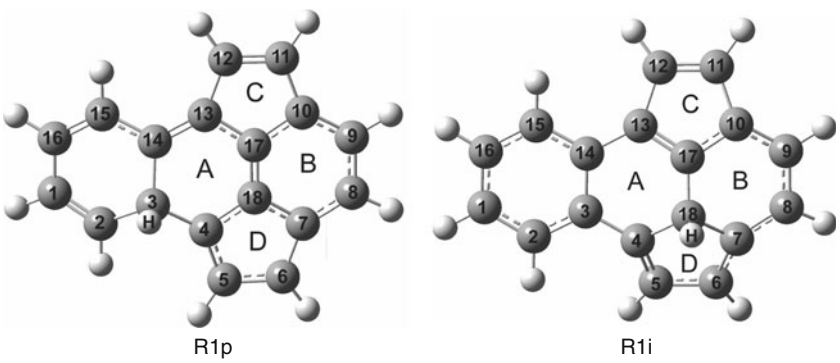

Fig. 2 The optimized geometries of the radicals under investigation

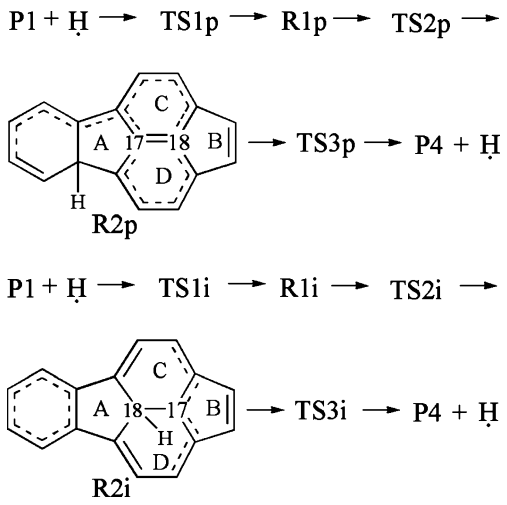

Fig. 3 Mechanism of the formation of R1p and R1i from dicyclopenta[*de,mn*]anthracene (P1) and hydrogen atom, their transformation in pathway A, and homolytic cleavage of the R2p and R2i radicals to acefluoranthene (P4) and hydrogen atom. TS1p, TS1i, TS2p, TS2i, TS3p, and TS3i denote transition states

formation of the C4–C17 and C10–C18 bonds occurs. The animation of the formation of R2p *via* TS2p, provided in Online Resource 3, clearly presents the concerted dyotropic rearrangement of C17 and C18. NBO analysis shows that the weak single C4–C18 bond still exists, whereas C4–C17 and C10–C18 bonds have already been formed, implying that C4, C17, and C18 form a 3-membered cycle. It is reasonable to expect that this 3-membered ring induces a significant strain in TS2p. Similarly, a simultaneous cleavage of the C7–C18 and C13–C17 bonds, and formation of the C7–C17 and C13–C18 bonds take place in TS2i. Here, the weak single C13–C17 bond still exists, whereas the C7–C17 bond has already been formed. The C4–C17 bond of TS2p and the C7–C17 bond of TS2i are

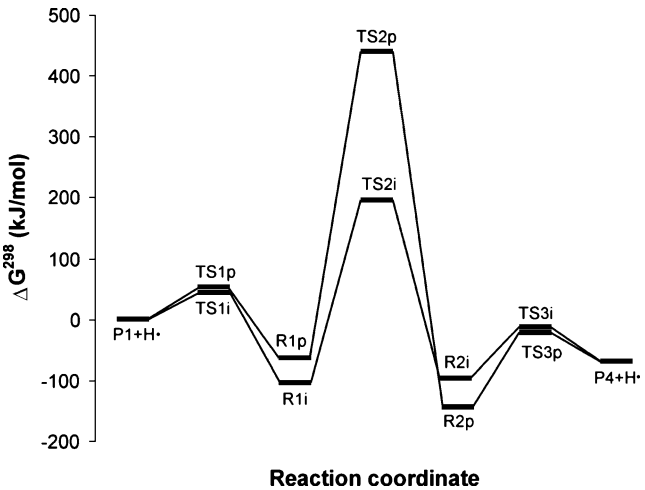

Fig. 4 Energy profile of the formation of the R1p and R1i radicals, and their transformation in pathway A. See Fig. 3 for definition of symbols

formed by the overlap of the corresponding p orbitals. The occupancies in the C4–C17 and C7–C17 NBOs are very low, and amount 1.56 and 1.60, respectively. These findings are in agreement with the corresponding bond distances (Table 1). According to the spin density, the unpaired electron is delocalized over the benzene moiety of TS2p (C2 – 0.345, C14 – 0.342, C16 – 0.454), whereas in TS2i spin density is distributed among C5 (0.160), C7 (0.238), C11 (0.327), and C13 (0.296), implying that the aromaticity of the benzene moiety is preserved. C17 of TS2p and C7 of TS2i are sp hybridized. In TS2i all other carbons are approximately sp^2 hybridized, but some bond angles and dihedral angles deviate from the values characteristic for sp^2 hybridized carbon lattices. As a consequence, C18 particularly deviates from planarity (*i.e.*, C18 lies outside the approximate plane spanned by the other carbon atoms). It is worth emphasizing that C18 also deviates from planarity in the starting R1i. In TS2p, the carbon atoms C3 and C18 are sp^3 hybridized, bonded to sp^2 and sp hybridized carbons. As a consequence of deviation from the usual dihedral bond angles, the sp hybridized C17 particularly deviates from planarity. It should be pointed out that in the starting R1p the pyracylene moiety consists of sp^2 hybridized carbons (excluding C3), and is essentially planar. All these facts imply that structural differences between TS2p and R1p are significantly more pronounced than they are between TS2i and R1i. These structural differences can be a reason for the fact that the activation barrier for the formation of TS2i (301.8 kJ mol^{-1} – Table 2 in Online Resource 1) is considerably lower than that for the formation of TS2p (505.0 kJ mol^{-1} – Table 1 in Online Resource 1).

The major feature of the intermediates R2p and R2i is that the rings A and B are 5-membered, whereas the rings C and D are 6-membered (Fig. 3 and Online Resource 2). The unpaired electrons reside in the delocalized SOMOs (Fig. 2 in Online Resource 1). The spin density maps of the radicals are in agreement with the NBO analysis, which shows that spin density is distributed among C2 (0.283), C8 (0.101), C10 (0.139), C12 (0.163), C14 (0.344), C16 (0.385), and H (0.051) in R2p, and among C4 (0.196), C6 (0.301), C11 (0.301), C13 (0.196), C17 (0.312), and H (0.105) in R2i.

The last step in pathway A, where the product P4 is formed, is cleavage of the C-H bond. This step occurs *via* transition states TS3p and TS3i (Figs. 3 and 4), and requires the activation barriers of 121.0, and 82.6 kJ mol^{-1}, respectively (Tables 1 and 2 in Online Resource 1). Since all carbon atoms are sp^2 hybridized, they almost lie within a plane (Fig. 3 and Online Resource 2). One can conclude, by inspecting α-density of both transition states, that the unpaired electrons reside in the s orbitals of H with noticeable low occupancies (0.89 in TS3p, and 0.88 in

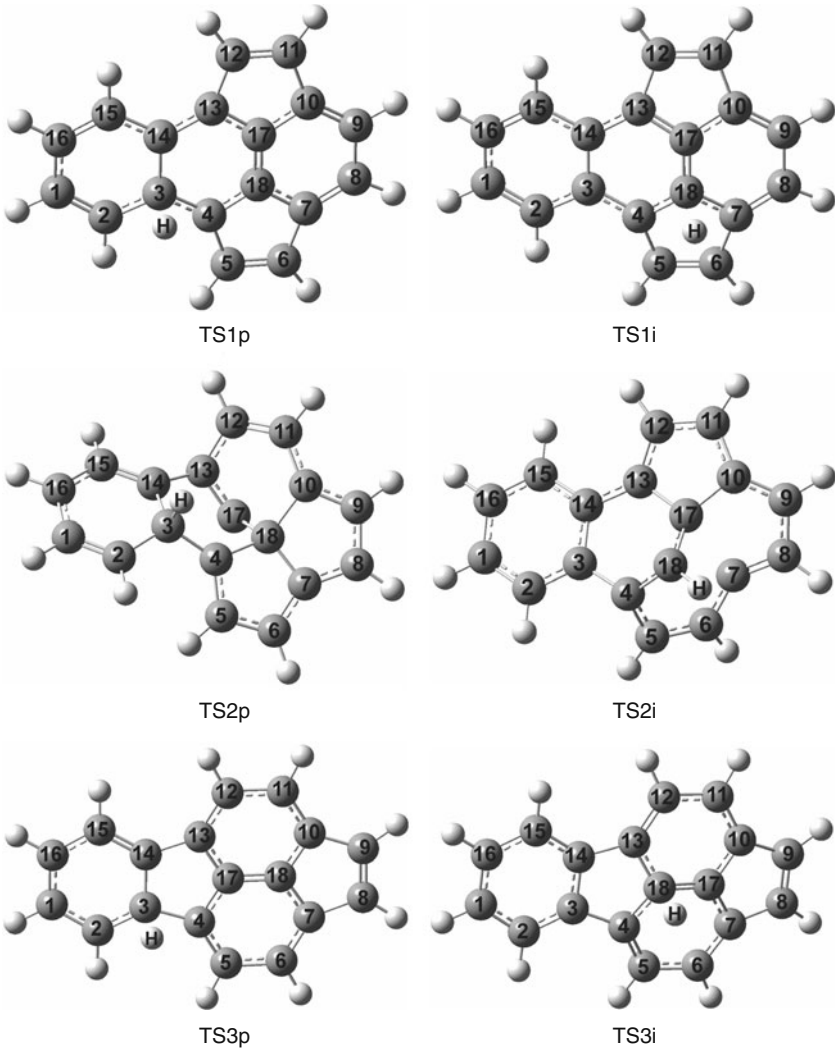

Fig. 5 The optimized geometries of the transition states participating in pathway A

TS3i). These low occupancies are due to donation of density from the s orbital of H to the antibonding π*(C3–C14) orbital in TS3p, and π*(C17–C18) orbital in TS3i.

The rate determining step in pathway A is the formation of TS2p and TS2i (Fig. 4). The activation energy for the reaction where a hydrogen atom is added to the external carbon is comparable to that for the corresponding isomerization of P1 [29]. The addition of a hydrogen atom to the internal carbon significantly lowers the activation barrier.

Pathway B

We now point out another mechanism for transformation of R1p and R1i to R2p and R2i. The scheme and energetic diagram of this mechanism are presented in Figs. 6 and 7. The optimized geometries of the transition states in pathway B are depicted in Fig. 8. The selected bond distances of the transition states and intermediate radicals are provided in Table 2, whereas the values of the total energies, enthalpies and free energies are given in Tables 3 and 4 in Online Resource 1.

A cleavage of the C17–C18 bond of R1p and R1i, followed by the simultaneous formation of the C7–C17 and C13–C18 bonds, was considered as the first step in pathway B (Figs. 6 and 7). The revealed transition states are shown in Fig. 8 and Online Resource 2. Both TS4p and TS4i are late transition states, and require the activation barriers of 487.9 and 274.5 kJ mol^{-1} (Tables 3 and 4 in Online Resource 1). In both cases, the weak C7–C17 bond already exists (Table 2). The NBO analysis of TS4i reveals that the C13–C18 bond has a noticeable low occupancy of 1.61. This bond is formed by the overlap of the p orbital of C13 and sp^3 orbital of C18. Bond angles that include C18 do not deviate significantly from those characteristic for sp^3 hybridized carbons. On the other hand, an inspection of the α-density of TS4p reveals a half bond between C13 and C18 with the occupancy of 0.79. This bond is formed by a partial overlap of the p orbital of C13 and sp^2 orbital of

Table 1 Bond distances that suffer significant changes in pathway A

Distance (Å)	P1	TS1p	R1p	TS2p	R2p	TS3p	P4
C2–C3	1.425	1.442	1.507	1.503	1.499	1.402	1.385
C3–C4	1.415	1.429	1.516	1.520	1.531	1.500	1.488
C3–C14	1.485	1.503	1.568	1.535	1.546	1.453	1.438
C3-H		1.828	1.112	1.109	1.110	1.869	
C4–C17	2.419	2.423	2.443	2.019	1.401	1.405	1.407
C4–C18	1.387	1.390	1.418	1.505	2.413	2.417	2.421
C10–C17	1.413	1.411	1.407	2.166	2.435	2.427	2.426
C10–C18	2.433	2.430	2.415	1.574	1.408	1.405	1.404
C17–C18	1.361	1.360	1.349	1.467	1.359	1.357	1.356
		TS1i	R1i	TS2i	R2i	TS3i	
C4–C18	1.387	1.401	1.487	1.409	1.504	1.427	1.407
C7–C17	2.433	2.445	2.472	2.028	1.398	1.402	1.404
C7–C18	1.413	1.432	1.493	2.151	2.515	2.442	2.426
C13–C17	1.387	1.380	1.360	1.480	2.462	2.431	2.421
C13–C18	2.419	2.429	2.488	2.450	1.504	1.427	1.407
C17–C18	1.361	1.376	1.451	1.420	1.456	1.375	1.356
C18-H		1.881	1.111	1.083	1.114	1.765	

C18. Bond angles that include C18 significantly deviate from those characteristic for sp^2 hybridized carbon atoms. This structural feature of TS4p, and the well-known fact that species with odd-electron bonds are usually highly reactive, could be a reason for the fact that G_{298} for TS2p is significantly higher than that for TS2i (Tables 3 and 4 in Online Resource 1), and requires a higher activation barrier.

In the intermediates Ip and Ii the rings A – D are all 5-membered, and there is a 4-membered cycle between the rings A and B (Fig. 6 and Online Resource 2). The structures of the intermediates are very similar to those of the preceding transition states, and thus, the stabilization of the systems is poor (Fig. 7, and Tables 3 and 4 in Online Resource 1). This particularly refers to Ii, which is formed by the stabilization of the transition state that already contains a 4-membered ring. Ip is significantly less stable than Ii, which can be explained with the pronounced deformation that causes the presence of the sp^2 hybridized C18 with the atypical bond angles and dihedral angles. As Fig. 3 in Online Resource 1 shows, the unpaired electrons are delocalized. The NBO analysis of the spin distribution is in agreement with the spin density maps. Namely, spin density is distributed among C2 (0.374), C14 (0.372), C16 (0.489), and H (0.081) in Ip, and between C4 (0.583), and C6 (0.339) in Ii.

A simultaneous cleavage of the C7–C18 and C13–C17 bonds, and formation of the C17–C18 bond of the intermediate radicals was examined as the last step in pathway B (Figs. 6 and 7). The early transition states TS5p and TS5i were found (Fig. 8 and Online Resource 2). As an illustration, the results of the IRC calculation for TS5i are presented in Fig. 3 in Online Resource 1. Since the structures of TS5p and TS5i are very similar to those of the preceding intermediates, they require very low activation energies of 28.8 and 7.5 kJ mol^{-1}, respectively

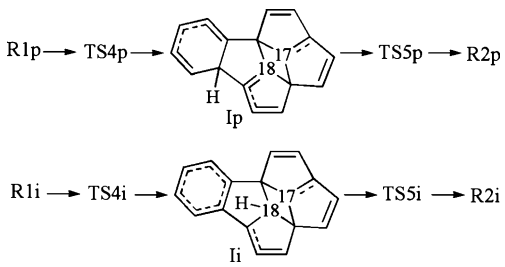

Fig. 6 Mechanism of the isomerization of R1p and R1i in pathway B. TS4p, TS4i, TS5p, and TSpi stand for transition states, whereas Ip and Ii denote intermediate radicals

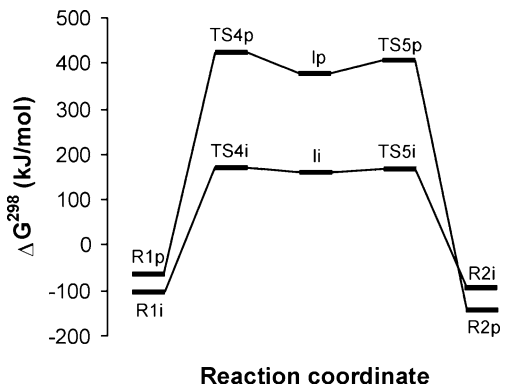

Fig. 7 Energy profile of the isomerization of R1p and R1i in pathway B. See Fig. 6 for definition of symbols

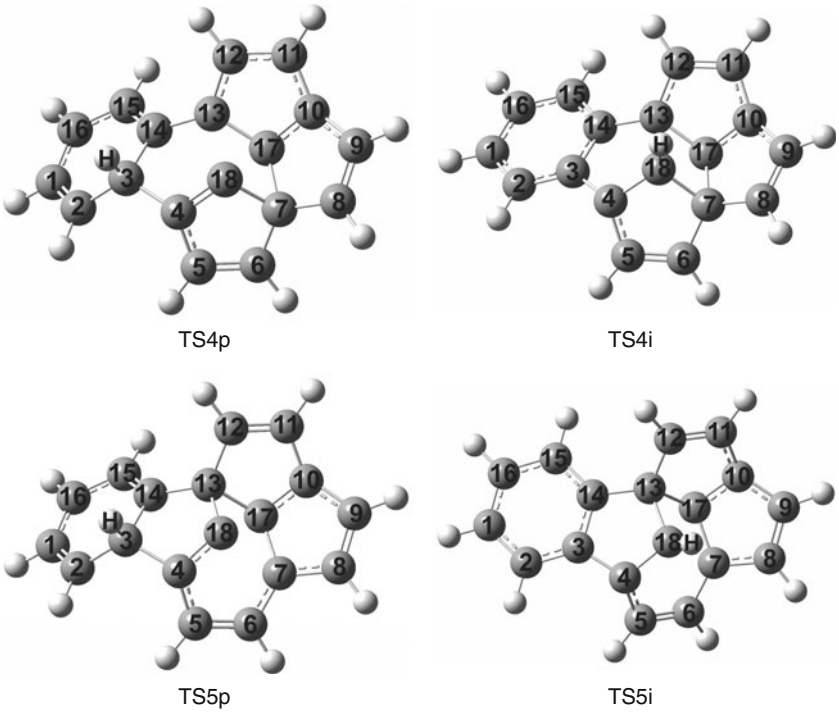

Fig. 8 The optimized geometries of the transition states participating in pathway B

(Tables 3 and 4 in Online Resource 1). The weak C13–C17 bonds still exist in the transition states (Table 2). NBO analysis reveals the existence of the weak C7–C17 bonds with the occupancies of 1.58 in TS5p, and 1.62 in TS5i. In TS5p this bond is formed by the overlap of the p orbital of C7 and the sp^2 orbital of C18. In TS5i the C7–C17 bond is formed by the overlap of the p orbital of C7 and the sp^3 orbital of C18. The energetic difference between the two transition states can again be attributed to the sp^2 hybridized C18 in TS5p, which forms the nonconforming bond angles and dihedral angles.

The rate determining step in pathway B is the formation of TS4p and TS4i (Fig. 7). As in the case of pathway A, the addition of hydrogen atom to the internal carbon significantly lowers the activation energy for hydrogen-mediated isomerization of P1 to P4. Though the B3LYP functional turned out to be successful in explaining the activation energy lowering, we need to point out that some long bonds are present in the transition states encountered in both types of transformation of the radicals R1p and R1i into R2p and R2i [38].

Summary

Our study examined the formation and transformation of two radicals issued from P1. The radical were obtained by adding hydrogen atom to an internal carbon atom (R1i) and to the perimeter of P1 (R1p). Two pathways for the transformations of the radicals to P4 + H· were revealed. Pathway A is a concerted rearrangement, whereas pathway B includes two transition states and a cyclobutyl intermediate. Pathway B is energetically more favorable in comparison to pathway A. In both pathways the activation energies for the reactions where hydrogen atoms are added to the external carbons are comparable to that for the corresponding isomerization of P1. Addition of hydrogen atoms to the internal carbons significantly lowers the activation energies for the isomerization of the radicals. This fact is explained on the basis of the unfavorable structures of the transition states and intermediates that are encountered in the isomerization of R1p.

Table 2 Bond distances that suffer significant changes in pathway B. Note that in R2p C17 and C18 are oriented as they are in R2i (Fig. 3)

Distance (Å)	R1p	TS4p	Ip	TS5p	R2p
C7–C17	2.420	1.575	1.573	1.508	1.404
C7–C18	1.409	1.531	1.575	1.963	2.430
C13–C17	1.434	1.501	1.549	1.554	2.429
C13–C18	2.458	1.947	1.563	1.504	1.418
C17–C18	1.349	1.660	1.877	1.744	1.359
	R1i	TS4i	Ii	TS5i	R2i
C7–C17	2.472	1.556	1.548	1.515	1.398
C7–C18	1.493	1.553	1.623	1.864	2.515
C13–C17	1.360	1.506	1.542	1.548	2.462
C13–C18	2.488	1.884	1.620	1.554	1.504
C17–C18	1.451	1.789	1.922	1.792	1.456

Acknowledgments This work is supported by the Ministry of science of Serbia, projects No 144015G and 142025.

References

1. Otero-Lobato MJ, Kaats-Richters VEM, Havenith RWA, Jenneskens LW, Seinen W (2004) Di-epoxides of the three isomeric dicyclopenta-fused pyrenes: ultimate mutagenic active agents. Mutat Res 564:39–50
2. Wang JS, He X, Mulder PPJ, Boere BB, Cornelisse J, Lugtenburg J, Busby WF (1999) Comparative tumorigenicity of the cyclopenta-fused polycyclic aromatic hydrocarbons aceanthrylene, dihydroaceanthrylene and acephenanthrylene in preweanling CD-1and BLU: Ha mouse bioassays. Carcinogenesis 20:1137–1141
3. Howard JB, Longwell JP, Marr JA, Pope CJ, Busby WF Jr, Lafleur AL, Taghizadeh K (1995) Effects of PAH isomerizations on mutagenicity of combustion products. Combust Flame 101:262–270
4. Scott LT, Necula A (1997) Thermal migration of an ethynyl group from one benzene ring to another by reversible vinylidene C-H insertion. Tetrahedron Lett 38:1877–1880
5. Sarobe M, Jenneskens LW, Wesseling J, Snoeijer JD, Zwikker JW, Wiersum UE (1997) Thermal interconversions of the $C_{16}H_{10}$ cyclopenta-fused polycyclic aromatic hydrocarbons fluoranthene, acephenanthrylene, and aceanthrylene revisited. Liebigs Ann/Recueil 6:1207–1213
6. Sarobe M, Kwint HC, Fleer T, Havenith RWA, Jenneskens LW, Vlietstra EJ, van Lenthe JH, Wesseling J (1999) Flash vacuum thermolysis of acenaphtho[1, 2-a]acenaphthylene, fluoranthene, benzo[k]- and benzo[j]fluoranthene – homolytic scission of carbon-carbon single bonds of internally fused cyclopenta moieties at T≥1100 °C. Eur J Org Chem 5:1191–1200
7. Necula A, Scott LT (2000) High temperature behavior of alternant and nonalternant polycyclic aromatic hydrocarbons. J Anal Appl Pyrol 54:65–87
8. Jenneskens LW, Sarobe M, Zwikker JW (1996) Thermal generation and (inter)conversion of (multi) cyclopenta-fused polycyclic aromatic hydrocarbons. Pure Appl Chem 68:219–224
9. Scott LT, Roelofs NH (1987) Benzene ring contractions at high temperatures. Evidence from the thermal interconversions of aceanthrylene, acephenanthrylene, and fluoranthene. J Am Chem Soc 109:5461–5465
10. Sarobe M, Jenneskens LW, Wesseling J, Wiersum UE (1997) High temperature gas phase syntheses of $C_{20}H_{12}$ cyclopenta-fused polycyclic aromatic hydrocarbons: benz[*l*]-acephenanthrylene and benz[*j*]acephenanthrylene and their selective rearrangement to benzo[*j*]fluoranthene. J Chem Soc Perkin Trans 2(4):703–708
11. Marsh ND, Wornat MJ (2004) Polycyclic aromatic hydrocarbons with five-membered rings: distributions within isomer families in experiments and computed equilibria. J Phys Chem A 108:5399–5407
12. Scott LT, Roelofs NH (1988) Benzenoid ring contractions in the thermal automerization of acenaphthylene. Tetrahedron Lett 29:6857–6860
13. Gutman I, Furtula B (2008) Cyclic conjugation in pyracylene. Polyc Arom Comp 28:136–142
14. Gutman I, Đurđević J (2008) Fluoranthene and its congeners - a graph theoretical study MATCH. Commun Math Comput Chem 60:659–670
15. Cioslowski J, Schimeczek M, Piskorz P, Moncrieff D (1999) Thermal rearrangement of ethynylarenes to cyclopentafused polycyclic aromatic hydrocarbons: an electronic structure study. J Am Chem Soc 121:3773–3778
16. Violi A, Sarofim AF, Truong TN (2001) Quantum mechanical study of molecular weight growth process by combination of aromatic molecules. Combust Flame 126:1506–1515
17. Tsefrikas VM, Scott LT (2006) Geodesic polyarenes by flash vacuum pyrolysis. Chem Rev 106:4868–4884
18. Marković S, Stanković S, Radenković S, Gutman I (2008) Electronic structure study of thermal intraconversions of some dicyclopenta-fused polycyclic aromatic compounds. J Chem Inf Model 48:1984–1989
19. Stanković S, Marković S, Radenković S, Gutman I (2009) Formation and isomerization of dicyclopenta[de, mn]anthracene. Electronic structure study. J Mol Model 15:953–958
20. Stone AJ, Wales DJ (1986) Theoretical studies of icosahedral C_{60} and some related species. Chem Phys Lett 128:501–503
21. Murry RL, Strout DL, Odon GK, Scuseria GE (1993) Role of sp^3 carbon and 7-membered rings in fullerene annealing and fragmentation. Nature 366:665–667
22. Balaban AT, Schmalz TG, Zhu H, Klein DJ (1996) Generalizations of the Stone-Wales rearrangement for cage compounds, including fullerenes. J Mol Struct: THEOCHEM 363:291–301
23. Scott LT (1996) Fragments of fullerenes: novel syntheses, structures and reactions. Pure Appl Chem 68:291–300
24. Eggen BR, Heggie MI, Jungnickel G, Latham CD, Jones R, Briddon PR (1996) Autocatalysis during fullerene growth. Science 272:87–89
25. Slanina Z, Zhao X, Uhlík F, Ozawa M, Osawa E (2000) Computational modeling of the elemental catalysis in the Stone-Wales fullerene rearrangements. J Organomet Chem 599:57–61
26. Alder RW, Harvey JN (2004) Radical-promoted Stone-Wales rearrangements. J Am Chem Soc 126:2490–2494
27. Slanina Z, Zhao X, Uhlík F, Adamowicz L, Lee S-L (2004) Computations of the catalytic effects in the Stone-Wales fullerene isomerizations: N and CN agents. Int J Quantum Chem 99:634–639
28. Nimlos MR, Filley J, McKinnon JT (2005) Hydrogen atom mediated Stone-Wales rearrangement of pyracyclene: a model for annealing in fullerene formation. J Phys Chem 109:9896–9903
29. Marković S, Stanković S, Radenković S, Gutman I (2009) Thermal isomerization in cyclopenta[*fg*]aceanthrylene. Monats Chem 140:153–156
30. Richter T, Howard JB (2000) Formation of polycyclic aromatic hydrocarbons and their growth to soot – a review of chemical reaction pathways. Prog Energy Combust Sci 26:565–608
31. Becke AD (1988) Density-functional exchange-energy approximation with correct asymptotic behavior. Phys Rev A 38:3098–3100
32. Lee C, Yang W, Parr RG (1988) Development of the Colle-Salvetti correlation-energy formula into a functional of the electron density. Phys Rev B 37:785–789
33. Becke AD (1993) Density-functional thermochemistry. II. The role of exact exchange. J Chem Phys 98:5648–5652
34. Frisch MJ, Trucks GW, Schlegel HB, Scuseria GE, Robb MA, Cheeseman JR, Zakrzewski VG, Montgomery JA Jr, Stratmann RE, Burant JC, Dapprich S, Millam JM, Daniels AD, Kudin KN, Strain MC, Farkas O, Tomasi J, Barone V, Cossi M, Cammi R, Mennucci B, Pomelli C, Adamo C, Clifford S, Ochterski J, Petersson GA, Ayala PY, Cui Q, Morokuma K, Malick AD, Rabuck KD, Raghavachari K, Foresman JB, Cioslowski J, Ortiz JV, Baboul AG, Stefanov BB, Liu G, Liashenko A, Piskorz P, Komaromi I, Gomperts R, Martin RL, Fox DJ, Keith T, Al-Laham

MA, Peng CY, Nanayakkara A, Challacombe M, Gill PMW, Johnson B, Chen W, Wong MW, Andres JL, Gonzalez C, Head-Gordon M, Replogle ES, Pople JA (2003) Gaussian 03, Revision E.01-SMP. Gaussian Inc, Pittsburgh, PA

35. Gonzalez C, Schlegel HB (1989) An improved algorithm for reaction path following. J Chem Phys 90:2154–2161
36. Foster JP, Weinhold F (1980) Natural hybrid orbitals. J Am Chem Soc 102:7211–7218
37. Glendening D, Badenhoop JK, Reed AE, Carpenter JE, Bohmann JA, Morales CM, Weinhold F, Copyright 1996–2001 by Board of Regents of the University of Wisconsin System
38. Zhao Y, Truhlar DG (2004) Hybrid meta density functional theory methods for thermochemistry, thermochemical kinetics, and non-covalent interactions: the MPW1B95 and MPWB1K models and comparative assessments for hydrogen bonding and van der Waals interactions. J Phys Chem A 108:6908–6918